Available online at www.sciencedirect.com
ScienceDirect
European Journal of Pharmaceutics and Biopharmaceutics 70 (2008) 116–126
European Journal of Pharmaceutics and Biopharmaceutics
www.elsevier.com/locate/ejpb

Research paper

Supramolecular organization and release properties of phospholipid-hyaluronan microparticles encapsulating dexamethasone

Carolina Gómez-Gaete [a,b], Nicolas Tsapis [a,*], Lídia Silva [a], Claudie Bourgaux [a], Madeleine Besnard [a], Amélie Bochot [a], Elias Fattal [a]

[a] *Faculté de Pharmacie, Univ Paris Sud, Châtenay-Malabry, France*
[b] *Facultad de Farmacia, Universidad de Concepción, Concepción, Chile*

Received 15 January 2008; accepted in revised form 17 April 2008
Available online 25 April 2008

Abstract

We describe the supramolecular organization of hybrid microparticles encapsulating dexamethasone (DXM) prepared by spray drying 1,2-Dipalmitoyl-sn-Glycero-3-Phosphocholine (DPPC) and hyaluronic acid (HA). The effect of DXM concentration on size distribution and encapsulation efficacy was evaluated as a function of HA concentration. In the absence of HA, DXM leads to a strong particle aggregation, whereas in the presence of HA, the aggregation is practically suppressed. DXM percentage of encapsulation is high ($95 \pm 6\%$), independently of composition. Drug-excipient interactions were analyzed by differential scanning calorimetry (DSC) and X-ray diffraction. DSC demonstrates that only a small fraction of DXM interacts with DPPC, whereas X-ray diffraction does not detect this interaction. Finally, *in vitro* release studies show that HA does not influence DXM release kinetics. In all cases, a burst release of DXM is observed during the first hour. Under sink conditions, powder concentration in the release medium governs the extent of the burst. Under non sink conditions, DXM release is mostly governed by DXM solubility in the release medium. In the dry microparticles, DXM is probably mostly in amorphous domains within the DPPC-HA matrix. Upon hydration, the majority of the drug is released and only a small amount of DXM interacts with DPPC.

Keywords: Microparticles; Spray drying; Dexamethasone; Hyaluronic acid; DPPC

1. Introduction

Dexamethasone has demonstrated to be an efficient anti-inflammatory drug in the treatment of acute and chronic posterior segment eye diseases such as uveitis [1] or affections that involve neovascularization, such as proliferative vitreoretinopathy and subretinal neovascularization [2,3]. Since the administration by systemic route of large quantities of dexamethasone can induce undesirable side effects, a local treatment is often preferred. However, corneal administration does not allow a sufficient drug passage to the posterior segment. Periocular injections can achieve therapeutic levels in the vitreous/retina, but may produce periocular fibrosis, globe perforation and ptosis [4]. In these conditions, a therapy allowing direct release of drugs into the vitreous is often required for the effective treatment of posterior segment diseases.

Direct injections of corticoids into the vitreous have been shown to provide therapeutic concentrations and minimize the systemic side effects [5,6]. However, large boluses and repeated intravitreal injections may be required to ensure therapeutic levels over an extended period of time, leading to a reduction of patient compliance or to an increased likelihood of complications such as vitreous hemorrhage or retinal detachment [7]. Devices like

* Corresponding author. Univ Paris Sud, UMR CNRS 8612, Faculté de Pharmacie, 5 Rue Jean-Baptiste Clément, 92296 Châtenay-Malabry, France. Fax: +33 146619334.
E-mail address: nicolas.tsapis@u-psud.fr (N. Tsapis).

0939-6411/$ - see front matter © 2008 Elsevier B.V. All rights reserved.
doi:10.1016/j.ejpb.2008.04.013

implants, developed to avoid repeated injections, offer an excellent alternative [8,9]. Nevertheless, their principal disadvantage is that a large surgical incision is required [10].

To overcome these problems, the incorporation of drugs within microparticles represents a therapeutic opportunity. Microparticles have the advantage to be injected with fine needles, to be elaborated with biodegradable materials and to enhance drug retention in the vitreal cavity [11].

Microparticles elaborated by solvent emulsion–evaporation method using polymers derived from lactic and glycolic acids (PLGA) have been the most frequently used due to their low ocular toxicity [12,13]. However, encapsulation of corticosteroids within particulate systems by traditional methods (emulsion/evaporation) is often not very efficient even using hydrophobic polymers [14–16]. As dexamethasone is a poorly soluble corticoid, the use of a lipophilic excipient in the formulation that may interact with dexamethasone and may therefore lead to a controlled release is necessary. A method favoring a better encapsulation efficiency should therefore be considered. Microparticles elaborated by spray drying have been studied as efficient drug carriers to protect the integrity, stability and functionality of corticoids [17,18]. This encapsulation method using excipients such as phospholipids have demonstrated a sufficient entrapment capacity for lipophilic compounds [19].

Phospholipids such as dipalmitoylphosphatidylcholine (DPPC) have been used mainly in spray-dried powders developed for pulmonary administration [20–22]. Although DPPC is biocompatible and biodegradable, only a few ocular formulations have used it [23]. Previous studies have demonstrated that a concentration of 33 mM of phospholipids is not toxic by intravitreal injection [24].

This work describes the elaboration of dexamethasone microparticles by spray-drying. Hyaluronic acid (HA), a polysaccharide present naturally in the vitreous cavity, has been used to improve the physical properties of the spray-dried powders and to potentially modulate the drug release as already reported by other authors [25,26]. The aim of this study was to encapsulate dexamethasone into DPPC-HA microparticles obtained by spray-drying, to study their supramolecular organization and to evaluate the influence of excipients on the *in vitro* release under *sink* and *non sink* conditions.

2. Materials and methods

2.1. Materials

Dexamethasone (DXM) was provided by Chemos GmbH (Germany), 1,2-dipalmitoyl-sn-glycero-3-phosphatidylcholine (DPPC) by Genzyme Pharmaceuticals (Switzerland) and hyaluronic acid, sodium salt 95% (HA) (MW = 1000 kDa) by Acros organics (USA). Fluoresceinamine, cyclohexyl isocyanide (purity > 98%), *N*-(2-hydroxyethyl) piperazine-*N*′-(2-ethanesulfonic acid) (Hepes), acetaldehyde, dimethyl sulfoxide (DMSO) and sodium chloride (NaCl) were provided by Sigma–Aldrich (Germany). L-α-phosphatidylethanolamine-*N*-(lissamine rhodamine B sulfonyl) (ammonium salt) (egg-transphosphatidylated, chicken) (noted LissRhod-PE) was purchased from Avanti Polar lipids (USA). Ethanol absolute in analytical grade and acetonitrile in high-performance liquid chromatography (HPLC) grade were obtained from Carlo Erba Reagents (France). Water was purified using a RIOS system from Millipore (France).

2.2. Fluorescein-labelling of hyaluronic acid

Fluorescein–hyaluronic acid (fl–HA) was prepared according to the method described by de Belder and Wik [27]. Briefly, 25 mg of HA was dissolved into 20 mL of water, and mixed with 20 mL of DMSO. Then 12.5 mg of fluoresceinamine in DMSO (0.25 mL) containing acetaldehyde (12.5 μL) and cyclohexyl isocyanide (12.5 μL) was added to the mixture and the pH adjusted to 4.5. The solution was protected from light and maintained at room temperature (20 °C) under stirring for 5 h. Fl–HA was then precipitated with 5 mL of a saturated NaCl solution and 400 mL of cold absolute ethanol and centrifuged at 947*g* for 3 min. Pellets were pooled into 25 mL of water, and added to 250 mL of cold absolute ethanol. Centrifugation was repeated twice, and the final pellet was resuspended into 12.5 mL water and dialyzed exhaustively against water for 32 h to remove the excess of reagents. The dialyzed solution was finally freeze-dried.

2.3. Microparticle preparation and yield calculation

Microparticles were obtained by spray-drying using a mini spray dryer BÜCHI B-191 (Flawil, Switzerland), which operates in a co-current mode and is equipped with a 0.7 mm diameter two-fluid nozzle. The spray-drying parameters such as air-flow rate, feed-flow rate, inlet temperature and aspiration were maintained constant as determined previously [28] (Table 1). DPPC and DXM were dissolved into ethanol and sodium hyaluronate into water. Ethanolic and aqueous solutions were then mixed at a ratio of 70/30 (v/v) prior to spray-drying and the mixture maintained under moderate stirring while fed into the spray-dryer. The final solid concentration in the solvent mixture was fixed at 2 g/L. Powder samples were stored at room temperature under vacuum in a

Table 1
Operational conditions used in spray-drying method

Spray-drying parameters	Operational conditions
Feed-flow rate (mL/min)	17
Inlet temperature (°C)	110
Outlet temperature (°C)	51–63
Aspiration setting (%)	100
Air-flow rate (L/h)	600

dessicator immediately after spray-drying to limit moisture uptake of the samples between production and testing. It has been shown in a previous work that environmental moisture leads to a modification of the supramolecular organization of chemicals within particles [28]. The yield was calculated as a percentage of the mass of the powder collected divided by the initial mass of solids in the solution prior to spray-drying.

2.4. Particle size distribution

The volume median geometric diameter (D_{50}) and the volume mean particle size (D[4.3]) of the powders were measured by light diffraction using a Mastersizer 2000 equipped with a Scirocco dry disperser (Malvern Instruments, France) at a dispersing pressure of 1 bar. The refractive index used was 1.5. Each sample was measured in triplicate.

2.5. Scanning electron microscopy

Scanning electron microscopy (SEM) was performed using a LEO1530 microscope (LEO Electron Microscopy Inc., Thornwood, USA) operating between 1 and 3 kV with a filament current of about 0.5 mA. Powder samples were deposited on carbon conductive double-sided tape (Euromedex, France) and were coated with a palladium–platinum layer of about 4 nm using a Cressington sputter-coater 208HR with a rotary planetary-tilt stage, equipped with a MTM-20 thickness controller.

2.6. Fluorescence microscopy

LissRhod-PE was added to the ethanolic solution of DPPC to label lipids prior to mixing and spray-drying. Fl–HA was added to the HA aqueous solution to label HA prior to mixing and spray-drying. Typically, about 5 mg of LissRhod-PE and 10 mg of fl–HA were used for a 500 mL solution. Samples in suspension (Hepes) were placed between glass slides and observed right after hydration with a Leitz Diaplan microscope equipped with a Coolsnap ES camera (Roper Scientific, France). Green fluorescence (fl–HA) was observed with a 505–550 nm band-pass emission filter with excitation at 488 nm. Red fluorescence (LissRhod-PE) was observed with a long-pass 560 nm emission filter with excitation at 543 nm.

2.7. Confocal microscopy

LissRhod-PE was added to DPPC ethanolic solution and fl–HA to HA aqueous solution prior to mixing and spray-drying. Samples in suspension (Hepes) were placed between glass slides and observed right after hydration with a Zeiss LSM-510 confocal scanning laser microscope equipped with a 1 mW helium neon laser and an Argon laser, using a Plan Apochromat 63X objective (NA 1.40, oil immersion). Green fluorescence (fl–HA) was observed with a 505–550 nm band-pass emission filter under 488-nm laser illumination. Red fluorescence (LissRhod-PE) was observed with a long-pass 560-nm emission filter under 543-nm laser illumination. The pinhole diameter was set at 104 μm. Stacks of images were collected every 0.8 μm along the z axis.

2.8. Dexamethasone loading within microparticles

Around 2 mg of the spray-dried powder was exactly weighed and dissolved into 20 mL ethanol. After vortexing (3 min), a centrifugation (9030g, 10 min) was performed to eliminate the fraction of HA that was not soluble in ethanol. Then, 1 mL of the supernatant was vortexed with 1 mL acetonitrile and finally the solution was filtered through a 0.45 μm PolyVinylidine DiFluoride (PVDF) filter. The quantity of DXM in the microparticles was determined by injecting 20 μL of the filtered solution into a Waters™ liquid chromatograph (HPLC) equipped with a Waters™ 600 pump, a Waters™ 7956 interface, a Waters™ 2996 photodiode array detector, a Waters™ 717 autosampler and a Waters™ Empower Login software. The analysis was performed at 238 nm using an Interchrom Reverse Phase Nucleosil 5 C18 column (150 × 4.0 mm) with a mobile phase composed of 40% acetonitrile and 60% water at 1 mL/min. All the analysis was performed at room temperature. The method shows satisfactory linearity between 0.3 and 26 μg/mL ($r^2 = 0.9995$). Experiments were performed at least in duplicate for each formulation.

2.9. In vitro release kinetics of dexamethasone

In vitro release of DXM from microparticles was carried out under two types of conditions. Some experiments were performed under *sink conditions* where drug concentration in the medium was kept at least 4× lower than the solubility of DXM in Hepes buffer (100 μg/mL). Other experiments were performed under *non sink conditions* to be close from DXM concentrations used in other formulations being developed (15–175 μg/mL) [29,30]. An accurate quantity of sample was weighed and resuspended into 10 mM Hepes buffer saline (150 mM NaCl, pH 7.4) using a gentle vortex. A microcentrifuge tube was prepared for each time point, protected from light and kept at 37 °C under tangential stirring (150 rpm) (Heidolph-Titramax 1000, Germany). At predetermined time intervals, 400 μL of release medium was removed after centrifugation at 9030g for 10 min (Mini Spin Eppendorf centrifuge) and mixed with 600 μL of acetonitrile. A centrifugation (9030g, 10 min) was performed to eliminate HA which was not soluble in acetonitrile. After filtration (0.45 μm PVDF filter), samples were stored at 4 °C until analysis by HPLC as described above. DXM stability in Hepes at 4 °C for 30 days was verified. Experiments were performed at least in duplicate.

2.10. Small-angle and wide-angle X-ray scattering

X-ray experiments were performed with a fine-focus Cu anode source; Cu Kα ($\lambda = 1.54$ Å) radiation was selected and line focused by a multilayer mirror and collimated by slits. A microcalorimeter cell, MICROCALIX [31] was used as sample holder. Hydrated samples (10 mg/100 μL Hepes) were let to equilibrate for 12 h before X-ray experiments. Dry and hydrated samples were then loaded into Lindemann glass capillaries (diameter 1.5 mm) and maintained at 20 °C (dry and hydrated), 37 °C and 50 °C (hydrated samples only). Small-angle (SAXS) and wide-angle (WAXS) X-ray scattering patterns were recorded simultaneously using two position-sensitive linear gas detectors. The scattered intensity was reported as a function of the scattering vector $q = 4\pi\sin\theta/\lambda$, where θ is half the scattering angle and λ the wavelength. Detectors calibration was performed with the crystalline β form of highly pure tristearin as previously described [32].

2.11. Differential scanning calorimetry (DSC)

The DSC analysis was performed on hydrated samples on a differential scanning calorimeter (DSC7, Perkin-Elmer, USA). About 10 mg of powder was hydrated with 100 μL of Hepes 12 h before experiments. Then about 15 mg accurately weighed samples were loaded into 40 μL aluminum pans and analyzed. The DSC runs were conducted from 20 to 80 °C at a rate of 5 °C/min. Calibration was achieved using Indium ($T_{onset} = 156.60$ °C) as well as *n*-decane ($T_{onset} = -29.66$ °C). Experiments were performed at least in duplicate. Enthalpies were normalized with respect to DPPC weight in the sample.

3. Results and discussion

The aim of this work was to encapsulate dexamethasone into DPPC-HA microparticles obtained by spray-drying, to study their supramolecular organization and to evaluate the influence of excipients on the *in vitro* release under *sink* and *non sink* conditions. The spray-drying conditions, described above, were selected following a previous study related to the influence of hyaluronic acid on the morphology, structure and supramolecular organization of DPPC microparticles prepared by this process [28] (Table 1). It was shown that the addition of hyaluronic acid to the formulation leads to an increase of particle size and a decrease of aggregation due to a morphological change: pure DPPC particles are dense spheres whereas DPPC-HA microparticles are mostly hollow shells. This change arises from a modification of the Peclet number of the solution before spray-drying induced by the addition of HA [33,34].

In addition, at the supramolecular level, DPPC is organized according to an almost dry lamellar structure [35] where chains are stiff, fully extended, tilted with respect to the bilayer plane and organized according to a two dimensional hexagonal lattice within the bilayer plane. When HA is added, it is mostly "sandwiched" between bilayers with some hydrophobic segments inserted in between aliphatic chains [28]. The exact location of DXM in the supramolecular organization will be studied in detail since it may have some impact on drug release from microparticles.

3.1. Particle size distribution and morphology

The influence of DXM concentration was evaluated first in the absence of HA. Particle size distributions for 0% (top, red), 0.5% (top, green), and 10% DXM (top, blue) are presented in Fig. 1. Pure DPPC particles possess a size distribution presenting several peaks arising from aggregates of micron-sized particles (Fig. 1, top, red). For 0.5% DXM (w/w), the size distribution becomes bimodal with one peak around 10μm and another one around 100 μm (Fig. 1, top, green). As DXM concentration reaches 10% (w/w), the intensity of the 100μm peak increases and the distribution becomes almost unimodal. Theses changes can be attributed to particle aggregation: both the mean and the median sizes increase steeply as DXM is incorporated at a low concentration into the formulation (0.5%) (Fig. 1, bottom). The size increase is even accentuated for higher DXM concentrations. SEM images confirm laser diffraction results: one can observe rather spherical microparticles on the order of a few microns that

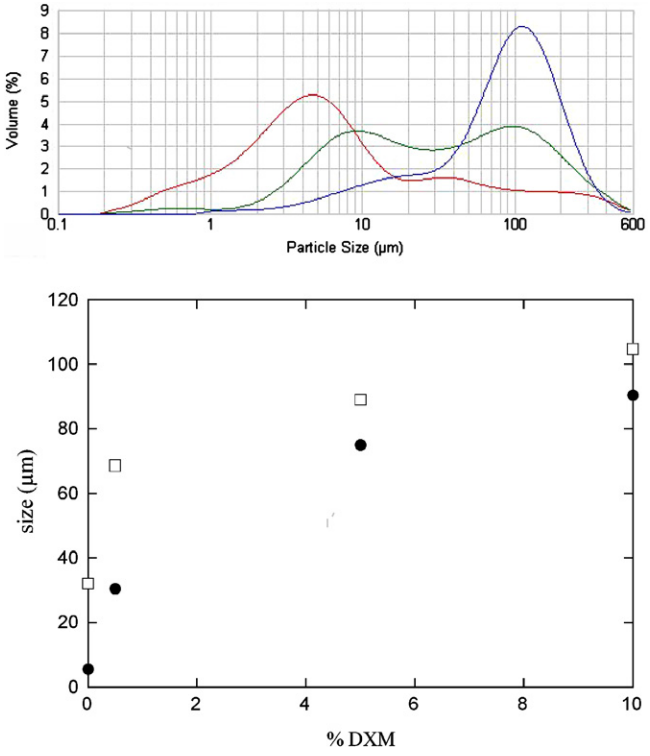

Fig. 1. Size distribution of spray-dried microparticles: pure DPPC microparticles (red), 99.5% w/w DPPC and 0.5% w/w DXM microparticles (green), 90% w/w DPPC and 10% w/w DXM microparticles (blue) (top). Volume weighed median diameter (●) and mean diameter (□) as a function of DXM concentration ($n = 3$, bottom).

form larger aggregates (Fig. 3A). For 10% DXM, micron-sized particles seem to have fused completely (Fig. 3D).

When 20% HA is present in the formulations, a bimodal size distribution is observed with a minor peak around 1.5 μm and a main one around 10 μm (Fig. 2, top). When DXM is incorporated, the distribution profile does not change with DXM concentration. The presence of the drug slightly increases the particle size (Fig. 2, bottom). SEM images reveal that the incorporation of DXM does not cause significant changes on the microparticle morphology. Particle morphology appears to be governed mostly by hyaluronic acid concentration. Qualitatively, DXM seems to induce an increase of aggregation, especially for large DXM concentrations in pure DPPC microparticles or microparticles containing 5% w/w of HA (Fig. 3B and E). On the other hand, DXM does not produce any visible effect on microparticle aggregation in the formulations with 20% HA (w/w) (Fig. 3C and F). These findings are in agreement with size distributions.

3.2. Yield and drug content

Powders were collected with a yield of about $35 \pm 7\%$ independently of DXM concentration. The drug however makes the powders more sticky. Encapsulation efficiencies were always very high, around $95 \pm 6\%$ ($n = 11$), without important differences relatively to the composition of the formulations. These encapsulation efficiencies are much higher than those obtained using the solvent emulsion/evaporation method and hydrophobic polymers [17].

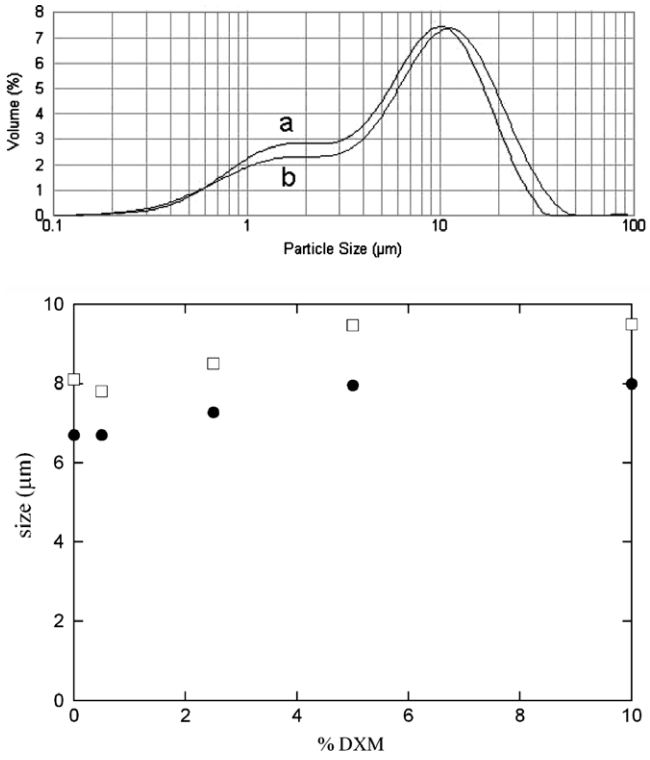

Fig. 2. Size distribution of spray-dried microparticles. (a) 80% w/w DPPC and 20% w/w HA microparticles, (b) 70% w/w DPPC, 20% w/w HA and 10% DXM microparticles (top). Volume weighed median diameter (●) and mean diameter (□) as a function of DXM concentration for microparticles contining 20% HA ($n = 3$, bottom).

3.3. Microscopy analysis

To better understand the behavior of the microparticles once suspended in the release medium, fluorescence and confocal microscopy were performed using double labelling. As described above, lipids were labelled with Liss-Rhod-PE (red), while HA was labelled with fluorescein (green). Previous experiments have shown that lipids and HA are homogeneously distributed within the shell of the dry microparticles [28].

Microparticles containing 20% w/w HA were hydrated with Hepes buffer (5 mg/mL). Samples were then imaged at predetermined time intervals (0.25, 1, 2, 4, and 6 h). As illustrated by Fig. 4, initially microparticles are perfectly spherical (0.25–1 h) and have a core shell organization with lipids mainly in the shell and HA in the core: upon hydration, some HA is quickly released outside and inside the particles. The green fluorescence is very bright within the core of the particle because HA is confined. After 2 h of incubation, microparticle's shells undergo deformation and become corrugated. Some microparticles even appear like they have exploded and released the inner HA in the outer environment. The tendency to HA expulsion is more marked after 4 and 6 h where most shells are broken. After particle explosion (6 h), the red fluorescence remains in the shell wall and is colocalized with the green fluorescence, meaning that some HA remains associated to the lipidic shell. Confocal microscopy confirms the fluorescence results. After HA expulsion, microparticle shell is of relatively homogeneous thickness and both components are uniformly distributed within the shell (Fig. 4B). Microparticle explosion probably arises from an osmotic pressure effect to equilibrate HA concentration inside and outside the shells.

3.4. Differential scanning calorimetry

DSC was performed on hydrated samples to assess the possible interactions between DPPC and DXM (0.5% and 10%) that might influence drug release. The thermogram of pure DPPC microparticles shows the typical pretransition corresponding to the conversion of the lamellar gel phase $L_{\beta'}$ into the ripple gel phase $P_{\beta'}$ and the main transition related to the passage from the $P_{\beta'}$ phase to the lamellar liquid-crystalline phase L_{α} (Fig. 5, left, curve a). The pretransition occurs at T_{onset} 37.2 °C with an enthalpy (ΔH) of 7 J/g of DPPC and the main phase transition at T_{onset} 42.1 °C with an enthalpy of ΔH of 41.1 J/g of DPPC. Thermograms are similar for DPPC-DXM microparticles (0.5% DXM): the main transition (T_{onset} and ΔH) is not modified (Fig. 5, left, b), however, the onset temperature and the ΔH of the pretransition decrease down to 34.5 °C and 5.5 J/g, respectively. On the other hand,

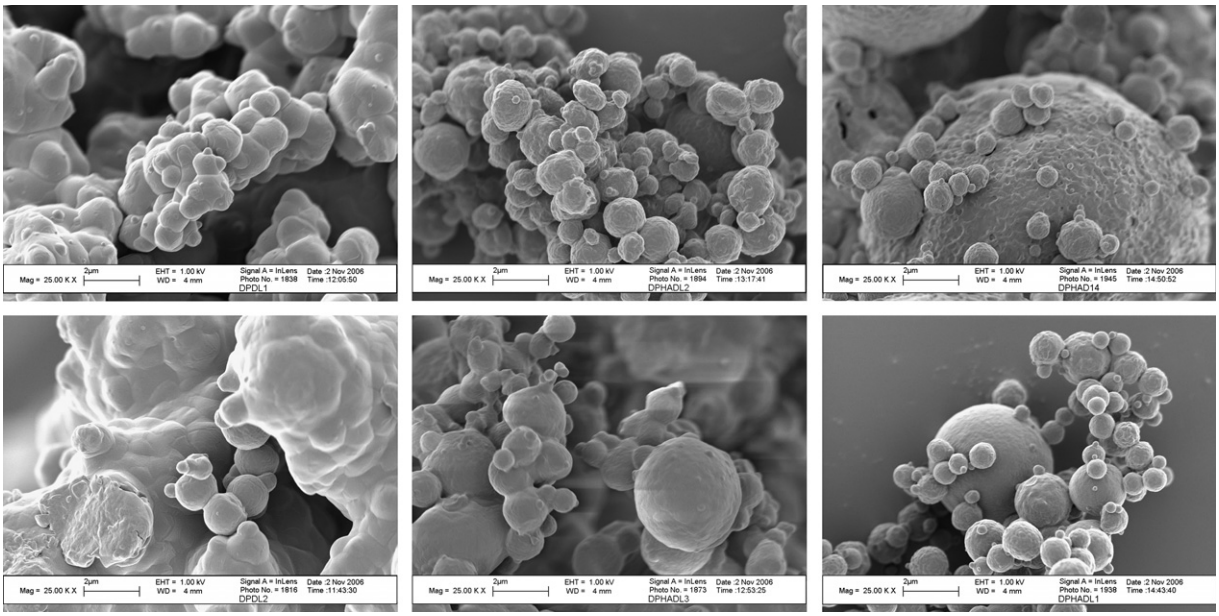

Fig. 3. SEM images of spray-dried powders: (A) 99.5% w/w DPPC and 0.5% w/w DXM microparticles, (B) 94.5% w/w DPPC, 5% HA and 0.5% w/w DXM microparticles, (C) 79.5% w/w DPPC, 20% w/w HA and 0.5% DXM microparticles, (D) 90% w/w DPPC and 10% w/w DXM microparticles, (E) 85% w/w DPPC, 5% HA and 10% w/w DXM microparticles, (F) 70% w/w DPPC, 20% HA and 10% w/w DXM microparticles. (scale bar = 2 μm).

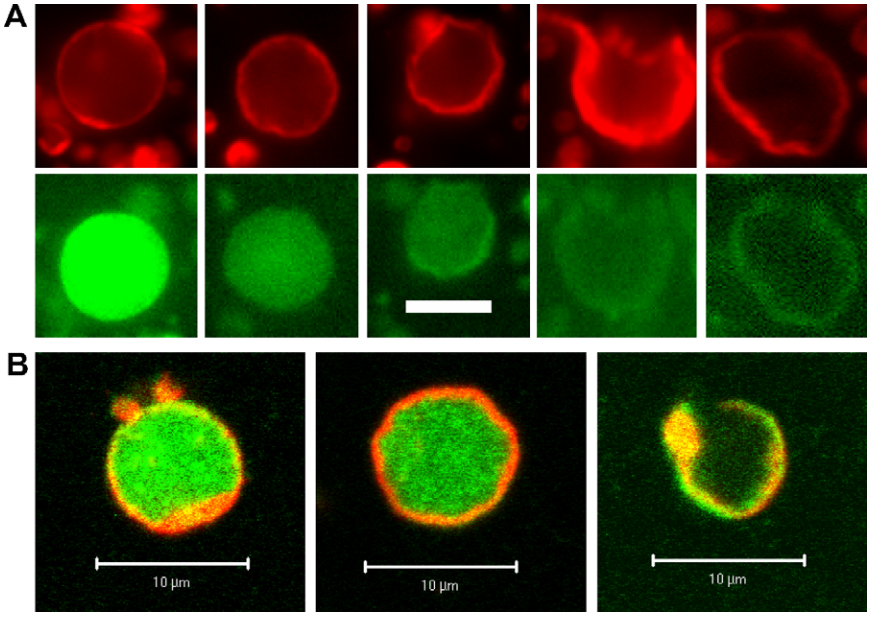

Fig. 4. (A) Fluorescence microscopy images of microparticles containing 80% w/w DPPC and 20% w/w HA in Hepes buffer. (Top) Red fluorescence (Rhod-PE). (Bottom) Green fluorescence (fl–HA). (scale bar = 10 μm). Each image correspond to a different time point: 0.25, 1, 2, 4 and 6 h from left to right. (B) Confocal microscopy images of microparticles containing 80% w/w DPPC and 20% w/w HA. Red fluorescence corresponds to LissRhod-PE and green fluorescence to fl–HA. From left to right, typical morphologies observed as microparticles are incubated in the buffer (scale bars = 10μm).

when 10% of DXM is incorporated to the formulation, the pretransition is almost abolished ($T_{onset} = 33.3$ °C and $\Delta H = 1.9$ J/g) and the onset temperature of the main transition is not modified, whereas the enthalpy decreases down to 32.4 J/g. (Fig. 5, left, curve c). The pretransition of DPPC, which is very sensitive to insertion of various small molecules within the bilayer [36], or adsorption on the bilayer, is suppressed in the presence of DXM. This behavior is common with that encountered with other molecules or drugs interacting with lipids like endosulfan [37], several carotenoids [38], progesterone [39] or tamoxifen [40]. In addition, the enthalpy of the main transition decreases with DXM concentration. Altogether these results prove the insertion of DXM within the bilayer.

The effect of DXM on the transitions of DPPC in formulations containing HA (20%) was also evaluated. The

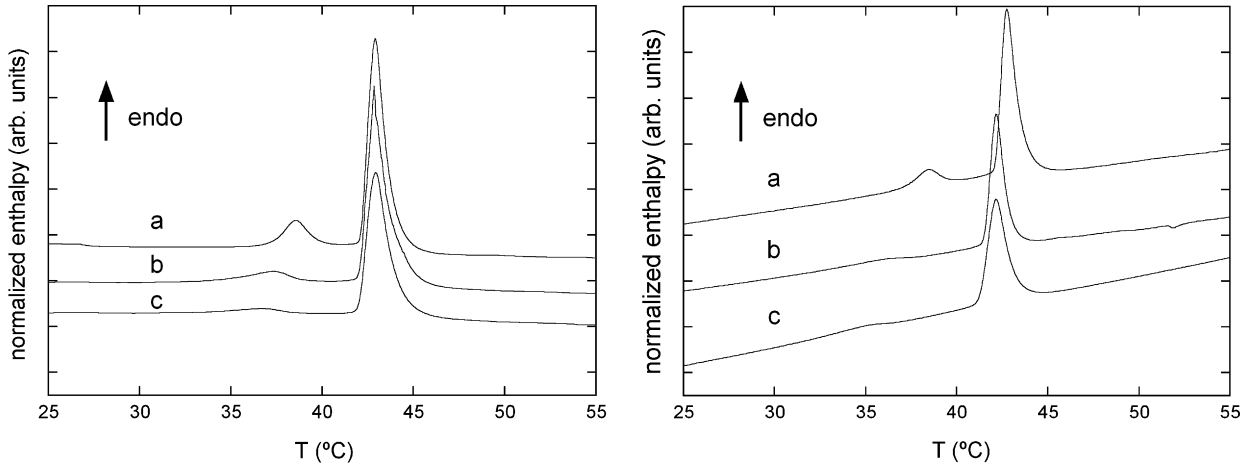

Fig. 5. DSC thermograms obtained from hydrated powders upon heating at 5 °C/min. left: (a) pure DPPC microparticles, (b) 99.5% w/w DPPC and 0.5% w/w DXM, (c) 90% w/w DPPC and 10% DXM. Right: (a) 80% w/w DPPC and 20% w/w HA, (b) 79.5% w/w DPPC, 20% w/w HA and 0.5% DXM, (c) 70% w/w DPPC, 20% w/w HA and 10% DXM.

thermogram of HA-DPPC microparticles is very similar to the pure DPPC microparticles. The pretransition occurs at T_{onset} 37.2 °C with an enthalpy (ΔH) of 6.2 J/g of DPPC and the main phase transition at T_{onset} 42.1 °C with an enthalpy of ΔH of 41 J/g of DPPC. The addition of DXM (0.5% and 10%) leads to a shift of the pretransition which is practically suppressed ($\Delta H \sim 2.6$ J/g). One can also observe a slight shift on the onset temperature of the main transition ($T_{onset} \sim 41$ °C) whereas the enthalpy is not modified. This suggests that in the presence of HA, DXM does not interact the same way with the DPPC bilayer: DXM may not insert as deeply as without HA due to possible Hydrogen bounds between OH groups of the drug and COO^- groups of HA or to steric hindrance arising from polysaccharide chains.

3.5. X-rays scattering on dry and hydrated samples

To probe the supramolecular organization of the components in the microparticles, an X-ray scattering study was performed on dry and hydrated samples. From a previous study [28], the supramolecular organization of the dry particles is known: DPPC is organized into an almost dry lamellar structure. When HA is present, it is sandwiched in between polar heads of the DPPC bilayers, with some hydrophobic segments inserted in between aliphatic chains. Typical SAXS and WAXS spectra of dry powders of pure DPPC (±DXM) are presented in Fig. 6 (top, left). Surprisingly, the incorporation of dexamethasone in the formulation does not modify the X-ray spectra of dry samples. We hypothesize that the drying process is too fast for most of the DXM to interact with the phospholipids and insert in between aliphatic chains. DXM is probably mostly amorphous and dispersed between lamellar domains. When HA is added, no effect of dexamethasone can be observed on dry samples.

Since DPPC mesophases are very sensitive to insertion of molecules within phospholipid bilayers, interactions between DPPC and DXM were also assessed by X-ray experiments on hydrated samples. Independently of HA concentration, hydrated microparticles exhibit the typical sequence of DPPC phases: a lamellar gel phase $L_{\beta'}$ at 20 °C, followed by the ripple gel phase $P_{\beta'}$ at 37 °C and lamellar liquid-crystalline phase L_α at 50 °C. Typical SAXS and WAXS spectra are presented in Fig. 6 (top-right and bottom-left). At 20 °C, SAXS and WAXS peaks slightly broaden as a function of HA concentration. The same features are observed at 37 and 50 °C. As a conclusion, for hydrated samples, HA introduces some disorder in the DPPC mesophases and is mostly present in the aqueous compartment between bilayers with some hydrophobic segments inserted within the bilayer itself.

The effect of DXM on hydrated samples was then studied. Typical spectra at 20, 37 and 50 °C are presented in Fig. 6 (top-right and bottom). The addition of dexamethasone does not modify any of the SAXS spectra, even for large amounts. Neither the position, nor the shape of the DPPC WAXS peaks were modified upon DXM addition. Nevertheless, for 10% DXM, additional peaks were observed on the WAXS spectra at all temperatures (Fig. 6, bottom, right). These peaks arise from crystallites of DXM, observable by optical microscopy along with microparticles, immediately after hydration (non sink conditions). These crystallites appear because at 10% DXM, in the hydration conditions used for X-ray experiments, we are above the solubility limit of DXM. This confirms that the drying process is too fast for DXM to interact with DPPC and insert within the lipid bilayer as predicted. As suggested above, in the dry particles, DXM is probably in amorphous domains dispersed within the DPPC-HA matrix. Upon hydration, DXM is quickly released in the buffer and depending on its concentration either is fully solubilized or tends to crystallize. The X-ray results are in disagreement with DSC results that suggest that a small amount of DXM is inserted in the DPPC bilayer. Since DSC is more sensitive than X-ray diffraction to detect interactions between molecules, we can hypothesize that a

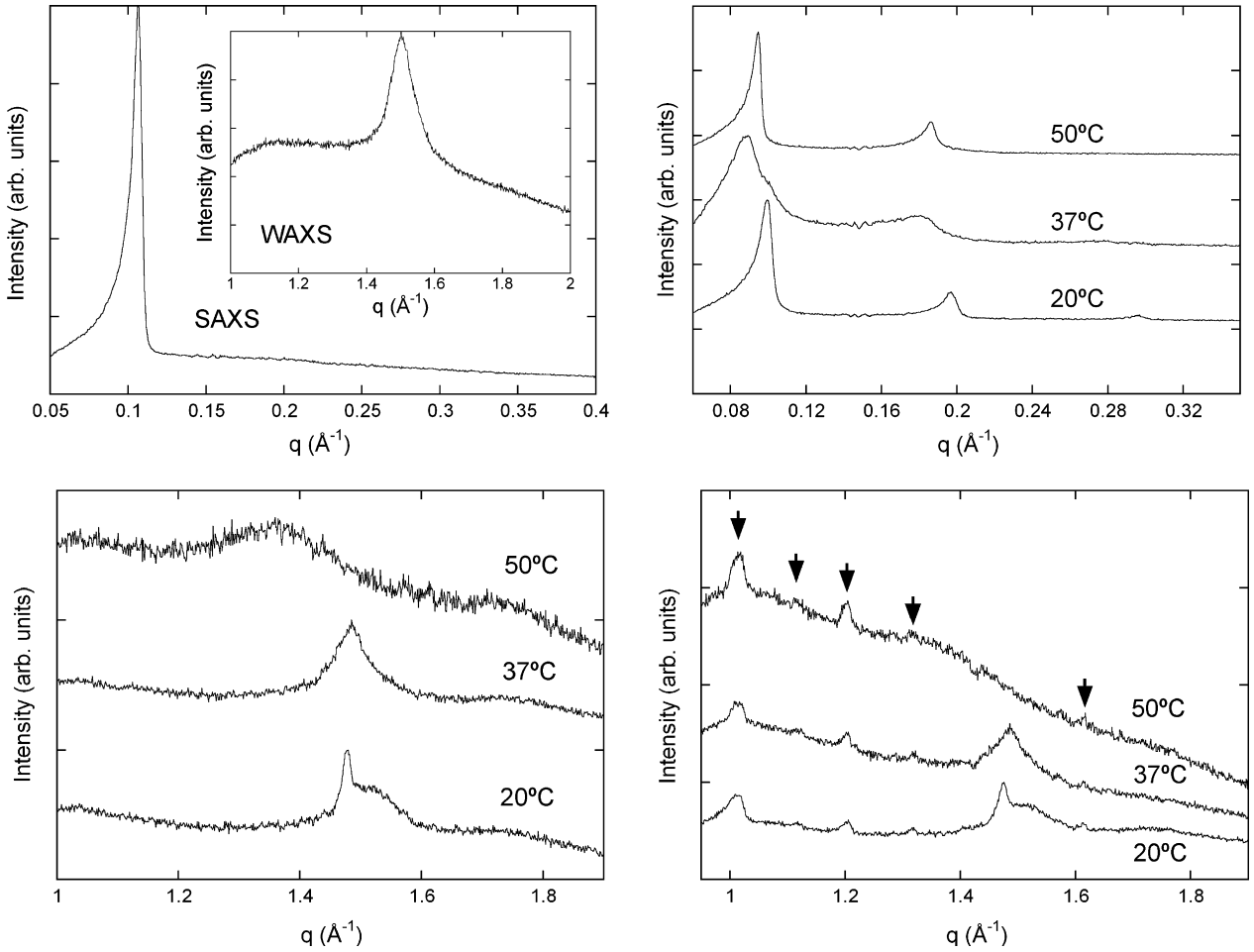

Fig. 6. (Top left) Typical SAXS and WAXS spectra of dry microparticles performed at 20 °C (here pure DPPC±DXM). (Top right) Typical SAXS spectra of hydrated samples presenting the characteristic features of the $L_{\beta'}$, $P_{\beta'}$ and L_{α} phases of DPPC, respectively, at 20, 37 and 50 °C. DXM addition does not modify the spectra. (Bottom left) Typical WAXS spectra of hydrated samples presenting the characteristic features of the $L_{\beta'}$, $P_{\beta'}$ and L_{α} phases of DPPC, respectively, at 20, 37 and 50 °C. 0.5% DXM does not modify these spectra. (Bottom right) Typical WAXS spectra of hydrated samples containing 10% DXM. The positions and shapes of the peaks arising from DPPC are not modified. However, several additional peaks appear independently of the temperature (arrows). These peaks arise from crystallites of DXM that coexist with microparticles.

rather small quantity of DXM is incorporated within the DPPC bilayer, the rest being free or crystallized.

3.6. In vitro release studies

Four *in vitro* release studies were performed. Table 2 shows the different proportions from each component in the formulations used for these studies.

The release profile of DXM from microparticles was first evaluated as a function of HA proportion (0%, 5%, 20% w/w). The amount of dexamethasone in the formulation was maintained constant (0.5% w/w), as well as the powder concentration for each time point (5 mg/mL buffer Hepes) (Table 2A). Similar release profiles were obtained independently of HA concentration (Fig. 7(a)). A burst release during the first hour was observed, followed by a plateau for which only around 50% of DXM was released during the time of study (24 h). HA does not favor a sustained release, on the contrary to what was observed by other authors [25]. Even if hydrogen bounds may exist between HA and DXM, they are probably weak as compared with DPPC/DXM interactions. We believe that DPPC/DXM interactions may govern drug release from the particles.

DXM release was then evaluated as a function of DXM concentration, for a fixed concentration of HA (20% w/w). Formulations containing 0.5%, 2.5% and 10% w/w of DXM were analyzed. For all experiments, the total DXM concentration in buffer Hepes was kept inferior to 10 μg/mL, in order to be under *sink conditions* (Table 2B). It implies using different powder concentration for each studied formulation. No differences were observed between the three formulations (Fig. 7(b)). The release behavior of DXM was characterized by a burst release during the first hour, which corresponds to almost 90% of drug encapsulated. These results differ from those obtained in the first study (DXM release as a function of HA concentration), where the maximal release of DXM was around 50%. The possible explanation of this discrepancy might arise from the difference in powder concentration in each

Table 2
Proportions of the different components of the formulations used for the DXM release studies

Study	% in the formulation			mg/mL Hepes			Total mass (mg/mL Hepes)
	DPPC	HA	DXM	DPPC	HA	DXM	
A	99.5	**0**	0.5	4.98	0.00	0.025	5.00
	94.5	**5**	0.5	4.78	0.25	0.025	5.00
	79.5	**20**	0.5	3.98	1.00	0.025	5.00
B	79.5	20	**0.5**	0.40	0.10	0.0025	0.50
	77.5	20	**2.5**	0.31	0.08	0.0100	0.40
	70.0	20	**10.0**	0.07	0.02	0.0100	0.10
C	79.5	20	0.5	0.40	0.1	0.0025	**0.50**
	79.5	20	0.5	0.80	0.2	0.0050	**1.00**
	79.5	20	0.5	1.59	0.4	0.0100	**2.00**
	79.5	20	0.5	3.98	1.0	0.0250	**5.00**
D	90	**0**	10	4.5	0	0.5	5
	80	**10**	10	4.0	0.5	0.5	5
	70	**20**	10	3.5	1.0	0.5	5

Bold entries indicate the parameters that has been modified for each study.
(A) Influence of HA on DXM release.
(B) Influence of DXM concentration on DXM release.
(C) Influence of powder concentration on DXM release.
(D) DXM release under *non sink* conditions.

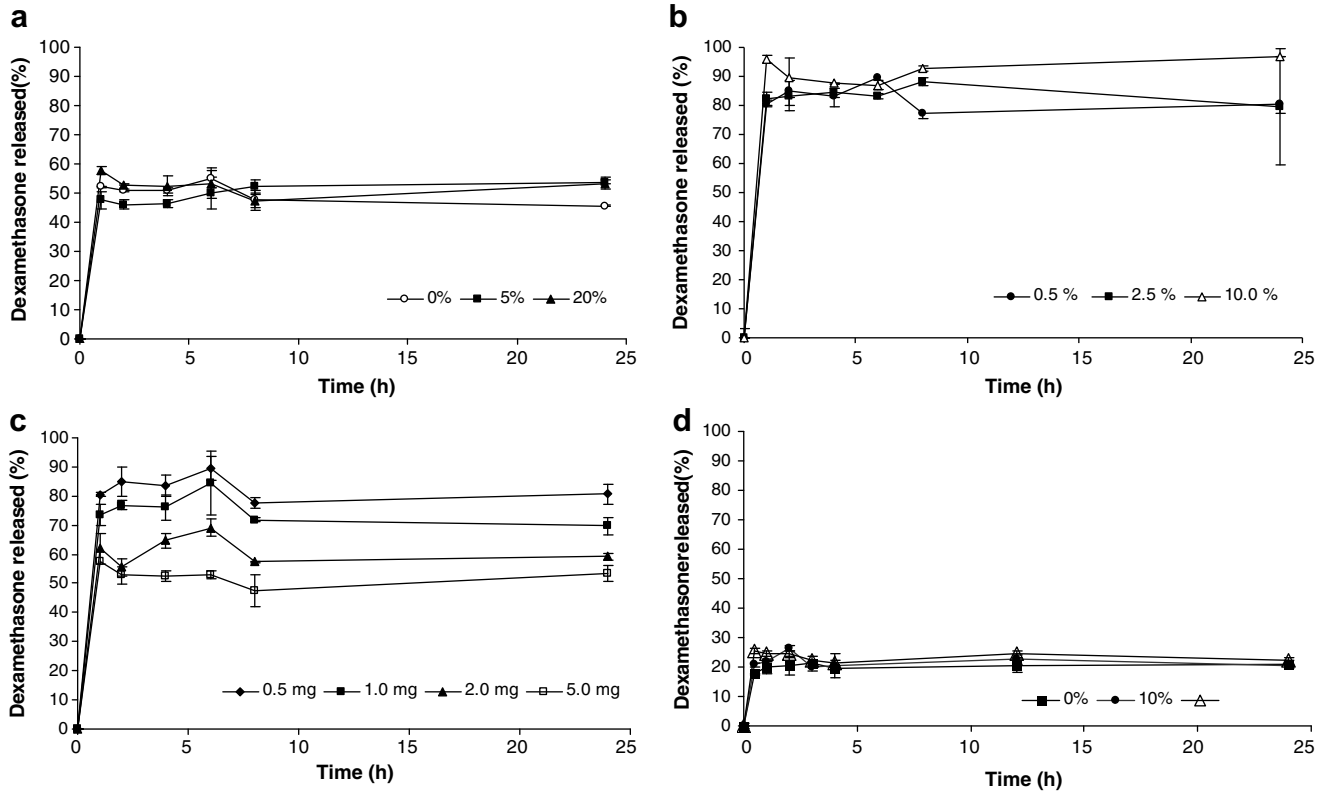

Fig. 7. *In vitro* DXM release from microparticles as a function of time. *Sink conditions*: (a) Effect of HA concentration: 0%, 5% and 20% w/w microparticles, (b) Effect DXM concentration: 0.5%, 2.5% and 10% w/w microparticles, (c) Effect of powder concentration: 0.5%, 1.0%, 2.0%, 5.0 mg/mL buffer Hepes (formulation containing 79.5% w/w DPPC, 20% w/w HA and 0.5% w/w DXM). Non sink conditions (final DXM concentration: 500 μg/mL): (d) formulation containing 10% w/w of DXM and different concentration of HA (0%, 10% and 20% w/w).

study (5 mg/mL in the first study, <0.5 mg/mL in the second) and not from DXM concentration since in all cases it is at least four times lower than the maximal solubility in Hepes.

In order to verify the later hypothesis, the effect of powder concentration in the release media was evaluated. The powder concentration was varied from 0.5 to 5 mg/mL (Table 2C), while a formulation containing 0.5% DXM

and 20% HA was used, in order to work under non saturation conditions. A burst release of DXM during the first hour was observed for all powder concentrations. However, the maximum drug released varies from 50% for 5 mg/mL to about 80–90% for 0.5 mg/mL (Fig. 7(c)). In the case of low powder concentration in the release medium (<1 mg/mL) the drug is probably released by diffusion from microparticles since DXM concentration in the particles is always superior to the concentration in the release medium. When powder concentration is higher than 2 mg/mL, the space between particles gets smaller, leading to the existence of a layer saturated with DXM around the particles. This layer might prevent DXM diffusion from microparticles and yield to the observed plateau.

Finally a release study under *non sink conditions* was performed. Formulations containing 10% w/w of DXM were used. The powder concentration was 5 mg/mL. The effect of different concentrations of HA was evaluated (0, 10 and 20% w/w). Similar profiles of DXM release were observed for all the formulations independent of HA concentration with a burst release corresponding to 20% of DXM during the first hours, followed by a plateau. The amount of DXM released at the plateau corresponds to the maximal solubility of DXM in Hepes (around 100 mg/mL): the buffer is saturated with DXM. This saturation is further confirmed by the observation of DXM crystallites along with microparticles in the release medium after 24 h at 37 °C.

Among all these release studies, the most interesting result corresponds to the first study performed under non saturation conditions (0.5% DXM w/w at 5 mg/mL: 25 μg/mL DXM): in this case only 50% of the drug is released during 24 h. This is not due to saturation since the total concentration of DXM is 4× below the solubility limit in Hepes. This effect arises from powder concentration as stated above.

4. Conclusion

We have encapsulated DXM within hybrid DPPC-HA microparticles prepared by spray-drying, and have studied the supramolecular organization of these microparticles and the effect of excipients on the release kinetics of DXM. Without HA, DXM addition leads to a strong particle aggregation which is not favorable for applications. In the presence of HA (5% and 20%), the aggregation effect of DXM is practically suppressed and one obtains rather monodisperse and well separated microparticles. DSC performed on hydrated samples shows that there is an interaction between DXM and DPPC. This interaction is different in the absence or presence of HA: DXM may incorporate partially within DPPC bilayers in the absence of HA while it only adsorbs on the bilayers in the presence of HA. X-ray experiments are not sensitive enough to detect these interactions confirming that a rather low amount of DXM interacts with DPPC. *In vitro* release studies show that HA does not modify the release kinetics of the hydrophobic drug. In all cases, a burst release of DXM is observed during the first hour. Under non saturation conditions, powder concentration in the release medium governs the extent of the burst: the lower the powder concentration (1 mg/mL<), the higher the burst effect (90%). Under non sink conditions, DXM release is governed by DXM solubility in the release medium. This case is not favorable for ocular applications since once released DXM quickly crystallizes. We believe that the interaction of DXM with DPPC is not favored by the fast drying process. In the dry microparticles DXM is probably mostly in amorphous domains within the DPPC matrix. Upon hydration, the majority of the drug is released and might eventually crystallize and a small amount of DXM interacts with DPPC. Since spray drying is known to favor drug amorphization, to obtain sustained release one should choose excipients that interact strongly with the drug. A more hydrophobic form of dexamethasone may have such properties and lead to sustained release.

Acknowledgements

C.Gómez-Gaete fellowship was supported by MECESUP Project UCO 0202 Ministerio de Educación, Chile and Universidad de Concepción, Chile. The authors acknowledge financial support from ANR Jeunes Chercheurs (ANR05-JC42284) thank A. Allavena-Valette (CECM, Vitry [s]/Seine) for access to the SEM facility, V. Nicolas for confocal microscopy (IFR 141-ITFM, Châtenay-Malabry) and M. Ollivon and K. Andrieux for fruitful discussions.

References

[1] S. Munoz-Fernandez, E. Martin-Mola, Uveitis, Best Pract. Res. Clin. Rheumatol. 20 (2006) 487–505.
[2] R. Machemer, G. Sugita, Y. Tano, Treatment of intraocular proliferations with intravitreal steroids, Trans. Am. Ophthalmol. Soc. 77 (1979) 171–180.
[3] T. Ishibashi, K. Miki, N. Sorgente, R. Patterson, S.J. Ryan, Effects of intravitreal administration of steroids on experimental subretinal neovascularization in the subhuman primate, Arch. Ophthalmol. 103 (1985) 708–711.
[4] P. Ferrante, A. Ramsey, C. Bunce, S. Lightman, Clinical trial to compare efficacy and side-effects of injection of posterior sub-Tenon triamcinolone versus orbital floor methylprednisolone in the management of posterior uveitis, Clin. Exp. Ophthalmol. 32 (2004) 563–568.
[5] S. Young, G. Larkin, M. Branley, S. Lightman, Safety and efficacy of intravitreal triamcinolone for cystoid macular oedema in uveitis, Clin. Exp. Ophthalmol. 29 (2001) 2–6.
[6] H. Tamura, K. Miyamoto, J. Kiryu, S. Miyahara, H. Katsuta, F. Hirose, K. Musashi, N. Yoshimura, Intravitreal injection of corticosteroid attenuates leukostasis and vascular leakage in experimental diabetic retina, Invest. Ophthalmol. Vis. Sci. 46 (2005) 1440–1444.
[7] G. Velez, S.M. Whitcup, New developments in sustained release drug delivery for the treatment of intraocular disease, Br. J. Ophthalmol. 83 (1999) 1225–1229.
[8] D.P. Hainsworth, P.A. Pearson, J.D. Conklin, P. Ashton, Sustained release intravitreal dexamethasone, J. Ocul. Pharmacol. Ther. 12 (1996) 57–63.

[9] G.J. Jaffe, D. Martin, D. Callanan, P.A. Pearson, B. Levy, T. Comstock, Fluocinolone acetonide implant (Retisert) for noninfectious posterior uveitis: thirty-four-week results of a multicenter randomized clinical study, Ophthalmology 113 (2006) 1020–1027.
[10] G.J. Jaffe, P.A. Pearson, P. Ashton, Dexamethasone sustained drug delivery implant for the treatment of severe uveitis, Retina 20 (2000) 402–403.
[11] C. Martinez-Sancho, R. Herrero-Vanrell, S. Negro, Poly (D,L-lactide-co-glycolide) microspheres for long-term intravitreal delivery of aciclovir: influence of fatty and non-fatty additives, J. Microencapsul. 20 (2003) 799–810.
[12] T. Moritera, Y. Ogura, Y. Honda, R. Wada, S.H. Hyon, Y. Ikada, Microspheres of biodegradable polymers as a drug-delivery system in the vitreous, Invest. Ophthalmol. Vis. Sci. 32 (1991) 1785–1790.
[13] R. Herrero-Vanrell, M.F. Refojo, Biodegradable microspheres for vitreoretinal drug delivery, Adv. Drug Deliv. Rev. 52 (2001) 5–16.
[14] T. Hickey, D. Kreutzer, D.J. Burgess, F. Moussy, Dexamethasone/PLGA microspheres for continuous delivery of an anti-inflammatory drug for implantable medical devices, Biomaterials 23 (2002) 1649–1656.
[15] I. Galeska, T.K. Kim, S.D. Patil, U. Bhardwaj, D. Chatttopadhyay, F. Papadimitrakopoulos, D.J. Burgess, Controlled release of dexamethasone from PLGA microspheres embedded within polyacid-containing PVA hydrogels, Aaps. J. 7 (2005) E231–E240.
[16] C. Gomez-Gaete, N. Tsapis, M. Besnard, A. Bochot, E. Fattal, Encapsulation of dexamethasone into biodegradable polymeric nanoparticles, Int. J. Pharm. 331 (2007) 153–159.
[17] P. Giunchedi, H.O. Alpar, U. Conte, PDLLA microspheres containing steroids: spray-drying, o/w and w/o/w emulsifications as preparation methods, J. Microencapsul. 15 (1998) 185–195.
[18] F. Pavanetto, I. Genta, P. Giunchedi, B. Conti, U. Conte, Spray-dried albumin microspheres for the intra-articular delivery of dexamethasone, J. Microencapsul. 11 (1994) 445–454.
[19] G. Colombo, R. Langer, D.S. Kohane, Effect of excipient composition on the biocompatibility of bupivacaine-containing microparticles at the sciatic nerve, J. Biomed. Mater. Res. A 68 (2004) 651–659.
[20] C. Bosquillon, C. Lombry, V. Preat, R. Vanbever, Influence of formulation excipients and physical characteristics of inhalation dry powders on their aerosolization performance, J. Control Release 70 (2001) 329–339.
[21] V. Codrons, F. Vanderbist, B. Ucakar, V. Preat, R. Vanbever, Impact of formulation and methods of pulmonary delivery on absorption of parathyroid hormone (1–34) from rat lungs, J. Pharm. Sci. 93 (2004) 1241–1252.
[22] C. Gervelas, A.L. Serandour, S. Geiger, G. Grillon, P. Fritsch, C. Taulelle, B. Le Gall, H. Benech, J.R. Deverre, E. Fattal, N. Tsapis, Direct lung delivery of a dry powder formulation of DTPA with improved aerosolization properties: effect on lung and systemic decorporation of plutonium, J. Control Release 118 (2007) 78–86.
[23] M.A. Ionita, R.M. Ion, B. Carstocea, Photochemical and photodynamic properties of vitamin B2-riboflavin and liposomes, Oftalmologia 58 (2003) 29–34.
[24] L. Lajavardi, A. Bochot, S. Camelo, B. Goldenberg, M.C. Naud, F. Behar-Cohen, E. Fattal, Y. de Kozak, Downregulation of endotoxin-induced uveitis by intravitreal injection of vasoactive intestinal Peptide encapsulated in liposomes, Invest. Ophthalmol. Vis. Sci. 48 (2007) 3230–3238.
[25] K. Surendrakumar, G.P. Martyn, E.C. Hodgers, M. Jansen, J.A. Blair, Sustained release of insulin from sodium hyaluronate based dry powder formulations after pulmonary delivery to beagle dogs, J. Control Release 91 (2003) 385–394.
[26] S.J. Kim, S.K. Hahn, M.J. Kim, D.H. Kim, Y.P. Lee, Development of a novel sustained release formulation of recombinant human growth hormone using sodium hyaluronate microparticles, J. Control Release 104 (2005) 323–335.
[27] A.N. de Belder, K.O. Wik, Preparation and properties of fluorescein-labelled hyaluronate, Carbohydr. Res. 44 (1975) 251–257.
[28] C. Gómez-Gaete, N. Tsapis, L. Silva, C. Bourgaux, E. Fattal, Morphology, structure and supramolecular organization of hybrid 1,2-dipalmitoyl-sn-glycero-3-phosphatidylcholine-hyaluronic acid microparticles prepared by spray drying, Eur. J. Pharm. Sci. (2008).
[29] M. Kodama, J. Numaga, A. Yoshida, T. Kaburaki, T. Oshika, Y. Fujino, G.S. Wu, N.A. Rao, H. Kawashima, Effects of a new dexamethasone-delivery system (Surodex) on experimental intraocular inflammation models, Graefes. Arch. Clin. Exp. Ophthalmol. 241 (2003) 927–933.
[30] R. Russell, Bioerodable eye implant may help treat macular edema, Pharmaceut. Sci. Technol. News (2003) 223–224.
[31] G. Keller, F. Lavigne, L. Forte, K. Andrieux, M. Dahim, C. Loisel, M. Ollivon, C. Bourgaux, P. Lesieur, DSC and X-ray diffraction coupling – specifications and applications, J. Thermal Anal. Calorimetry 51 (1998) 783–791.
[32] J.B. Brubach, V. Jannin, B. Mahler, C. Bourgaux, P. Lessieur, P. Roy, M. Ollivon, Structural and thermal characterization of glyceryl behenate by X-ray diffraction coupled to differential calorimetry and infrared spectroscopy, Int. J. Pharm. 336 (2007) 248–256.
[33] N. Tsapis, D. Bennett, B. Jackson, D.A. Weitz, D.A. Edwards, Trojan particles: large porous carriers of nanoparticles for drug delivery, Proceedings of the National Academy of Sciences of the United States of America 99 (2002) 12001–12005.
[34] N. Tsapis, E.R. Dufresne, S.S. Sinha, C.S. Riera, J.W. Hutchinson, L. Mahadevan, D.A. Weitz, Onset of buckling in drying droplets of colloidal suspensions, Phys. Rev. Lett. 94 (2005) 018302.
[35] A. Tardieu, V. Luzzati, F.C. Reman, Structure and polymorphism of the hydrocarbon chains of lipids: a study of lecithin–water phases, J. Mol. Biol. 75 (1973) 711–733.
[36] K. Lohner, Effects of small organic molecules on phospholipid phase transitions, Chem. Phys. Lipids 57 (1991) 341–362.
[37] R.A. Videira, M.C. Antunes-Madeira, V.M. Madeira, Biophysical perturbations induced by ethylazinphos in lipid membranes, Chem. Phys. Lipids 97 (1999) 139–153.
[38] A. Kostecka-Gugala, D. Latowski, K. Strzalka, Thermotropic phase behaviour of alpha-dipalmitoylphosphatidylcholine multibilayers is influenced to various extents by carotenoids containing different structural features – evidence from differential scanning calorimetry, Biochim. Biophys. Acta 1609 (2003) 193–202.
[39] F. Korkmaz, F. Severcan, Effect of progesterone on DPPC membrane: evidence for lateral phase separation and inverse action in lipid dynamics, Arch. Biochem. Biophys. 440 (2005) 141–147.
[40] M. Engelke, S. Tykhonova, M. Zorn-Kruppa, H. Diehl, Tamoxifen induces changes in the lipid composition of the retinal pigment epithelium cell line D407, Pharmacol. Toxicol. 91 (2002) 13–21.